HOLOGRAPHIC PHOTOTHERMOPLASTIC MEDIA BASED ON DONOR-ACCEPTOR SYSTEMS

N.A. DAVIDENKO, A.A. ISHCHENKO[1], L.I. KOSTENKO[2], N.G. KUVSHINSKY, D.A. MELENEVSKY, D.D. MYSYK[3], R.D. MYSYK[3], V.A. PAVLOV, N.G. CHUPRINA

Taras Shevchenko Kyiv National University
(64, Volodymyrs'ka Str., Kyiv 01033, Ukraine; e-mail: daviden@ukrpack.net),

[1]**Institute of Organic Chemistry, Nat. Acad. Sci. of Ukraine**
(5, Murmanska Str., Kyiv 02094, Ukraine; e-mail: alexish@i.com.ua),

[2]**Institute of Physical Organic and Coal Chemistry, Nat. Acad. Sci. of Ukraine**
(70, R.Luksemburg Str., Donetsk 8311, Ukraine),

[3]**Donetsk National Technical University**
(58, Artema Str., Donetsk 83000, Ukraine)

The main new informational characteristics of holographic recording photothermoplastic media based on films of poly-N-epoxycarbazole and the organic compound with intra- and intermolecular charge transfer are studied. Compounds with the intramolecular charge transfer from a donor to an acceptor through the system of π-bonds provide a greater holographic sensitivity and selectivity of absorption than compounds, for which the transfer occurs through space. In these recording media, the long-time latent image storage effect before the hologram development is discovered and explained.

Introduction

For the holographic interferometery and nondestructive check of the quality of metal constructions and machine details, the method of photo-thermoplastic hologram storage on a polymer film is used [1]. The latter should have small electroconductivity, high photoconductivity at the used wavelength of laser radiation, and plasticity. To storage a hologram, the holographic recording medium (RM) is prepared as a thin film applied on a electroconductive sublayer [1, 2]. Before the exposition, the free RM surface is charged in the corona discharge evenly. Therefore, because of its low conductivity, the high electric field is established between the electroconductive sublayer and the free surface. After the illumination of this film with the intensity-modulated light, the modulation of the surface charge originates from the photo-conductivity, and the latent image is created. The development of the latent image can be realized by the heating of the film to a softening temperature when the current electric pulse passes the sublayer. Within this process, the electrostatic forces of the latent image deform the film, and the latent image transforms to a geometric relief of the surface. To fix the holographic image, it is enough to cool the film to room temperature after the end of the pulse. The fixed image can be erased using the heating of the film to the surface leveling (healing) geometric relief temperature. In this case, the electric current pulse which passes the sublayer should be longer than the development pulse. After erasing the holographic image and cooling the film, it can be used for the next hologram storage. If the RM has a possibility to the long-time latent electrostatic image storage, then it can be used for the double-expose regime of the storage of holograms, when the expose takes place for the each hologram storage separately, but the development occurs simultaneously.

It is known that the RM films based on the poly-N-epoxypropylcarbozole (PEPC) contain organic acceptor additions [2, 3]. The centers of the light absorption and photogeneration of carriers in such films are intermolecular complexes with charge transition (CCT) [2]. In the case of the light quantum absorption, the transfer of an electron between the donor D (the PEPC carbazole fragment) and acceptor A (the acceptor molecule) takes place. After that, the valence electron from the next PEPC carbazole fragment can jump to a vacant molecular orbital of the carbazole fragment, which belongs to the CCT, i.e., there occurs the hole (electron vacancy) generation. The electron from the acceptor, which belongs to the CCT, can jump to the next acceptor molecule. The generated electron-hole pair (EHP) under the external electric field is separated into free charge carriers, which produces the photoconductive current [2, 4]. But the RM with the intermolecular CCT has a wide photosensitivity region in the whole

spectral range, which demands sometimes to employ the special methods for the RM protection from the outside illumination. Furthermore, these RMs have no possibility for the long-time latent image storage, which is an obstacle to use these in the double-expose hologram storage method [1]. In addition, the disadvantage of CCT as photogeneration centers is a small value of the absorption coefficient and its dependence, according to the RM informational characteristics, on the preparation conditions of polymer films. This fact yields that the CCT generation between the carbazole PEPC fragments and acceptor molecules proceeds as that in liquid solutions used for the film preparation, like in the formation of films when the solvent escapes [2].

Hence, it is more reasonable to use PEPC photoconductivity sensitizers with the narrow and intense-absorption region in the visible light range near the used laser wavelength. PEPC films with the organic compounds with intramolecular charge transfer (CICT) can be such RMs [2, 5, 6]. A CICT molecule consists of the D and A parts which are connected each with other by a chemical bond. The absorption coefficient of these polymer films doesn't depend on the preparation process unlike the film with CCT. When a light quantum is absorbed, then the electron transits from the D part to the A part of molecules. The fragments D and A can be or are covalently bounded by the insulating groups of atoms (type 1) [2, 5, 6] or a system of π-conjugated bonds (type 2) [7]. However, the comparative analysis of the informational characteristics of RM, containing the intermolecular CCT and CICT as photogeneration centers of the above-mentioned types was not made until now. Therefore, the goal of the present paper is such an analysis.

1. Samples and Experiment

The RM is based on PEPC + 1 mol.% TNF (TNF stands for 2,4,7-trinitro-9-florenon), compounds 1 and 2, 3—5. Compounds 1 and 2 refer to type 1, and compounds 3—5 to type 2. The structure formulas are listed below:

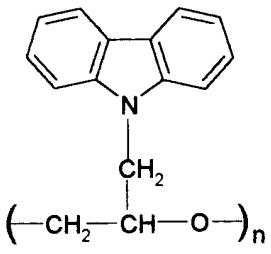

PEPC

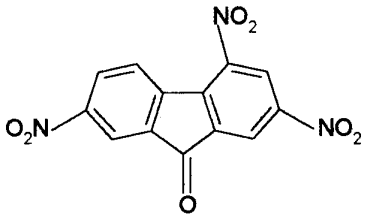

TNF

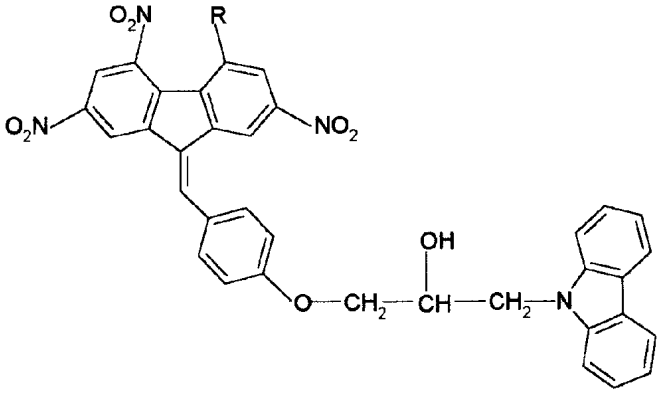

1 (CICT1), R = $COOCH_3$; 2 (CICT2), R = NO_2

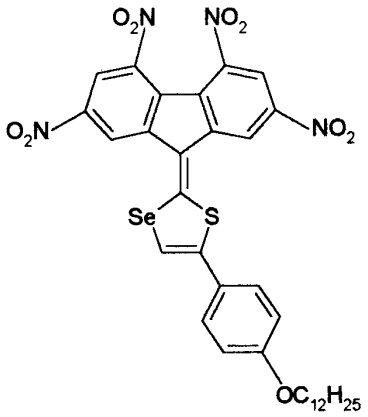

3 (CICT3)

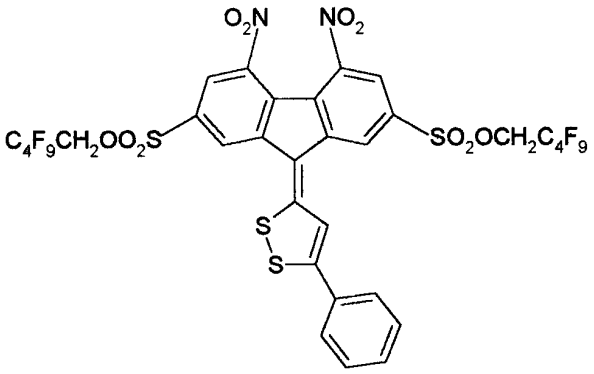

4(CICT4)

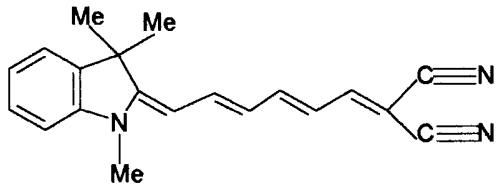

5 (MC)

The samples were prepared as a free surface structure (quartz substrate — polymer film) or as a structure (glass substrate — electroconductive layer SnO_2:In_2O_3 — polymer film). Polymer films were obtained as a result of the poured solutions PEPC + 1 mol.% (TNF, CICT1—CICT4, MC) in toluene on the substrates with or without a SnO_2:In_2O_3 layer. The thickness of the dried films was L=(1.1±0.05) μm, which is optimal for the hologram storage [2, 8].

In the samples with free-surface polymer films, the optical absorption spectra were measured in the wavelength range $\lambda = 400 \div 1000$ nm. To define the informational characteristics of the RM films prepared from PEPC+1 mol.% (TNF, CICT1—CICT4, MC), these films were applied on the glass substrates with 50×40 mm^2 dimensions, which were covered by a SnO_2:In_2O_3 sublayer with 20 Ω/mm^2 resistance and with two silver contacts on the opposite sides of the substrate. The working RM surface is 40×40 mm^2. To handle the storage hologram process, a special electronic device is used [2]. A maximal admissible value of the polymer film surface potential, while a local disruption of the polymer film doesn't occur, was defined for this device, as well as the optimal charging current value under the irradiation by positive ions. These values don't depend practically on the initial RM temperature in the temperature region 15 — 40 °C and are 125 V/μm and 1 μA/cm^2. Furthermore, the optimal temperature was automatically supported with the rate of above 10^6 grad/s.

We study the optimal spatial frequency range of the transfer linearity $\Delta\omega$, optimal spatial frequency of the transfer linearity ω_{opt}, holographic sensitivity S, the signal/noise ratio of the restored holographic image, the ratio of the intensities of the reference beam to the signal one on the hologram storage stage, and the recurrence and efficiency of the RM. To provide such investigations, the plane-wave front holograms were stored on a RM with the 633-nm wavelength of a He—Ne laser. The diffraction efficiency η in the 1st diffraction order was investigated by the detection with a photodetector. The photodetector was connected to an oscilloscope with the memory. The oscilloscope was synchronized with the leading front of a developing pulse. To define the maximal attainable value of η, the hologram developing was provided from the temperature $T = 293$ K up to the hologram erasing temperature, and the complete polymer film surface geometric relief was determined.

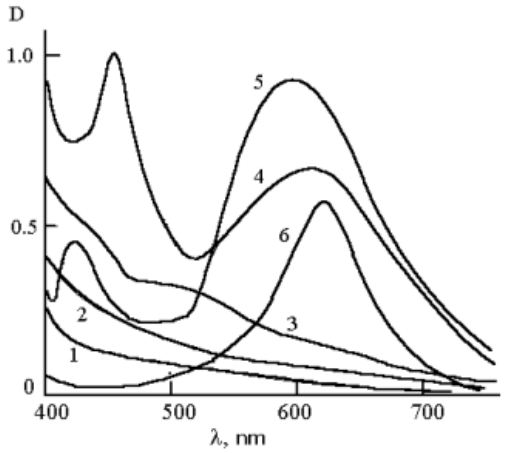

Fig. 1. Optical spectra of the films made of PEPC with 1 mol.% TNF (*1*), 1 (*2*), 2 (*3*), 3 (*4*), 4 (*5*), 5 (*6*)

2. Results and Discussion

Fig. 1 shows the absorption spectra of the investigated polymer films in the visible range. The absorption bands of the films with compounds 3—5 are found in a more long-wave area and have greater intensity (by more than one order) and selectivity in comparison with the intermolecular (PEPC:TNF) and intramolecular (compounds 1 and 2) bands of CCT (Fig. 1). This is caused by the fact that the intramolecular redistribution of charge over the system of easily polarized conjugate π-bonds for the former is accompanied by the much smaller energy consumption and a change of internuclear equilibrium distances under excitation, than that under the complete electron transfer through space for the latter.

The holograms of the plane wave front were obtained for the RM based on PEPC + 1 mol.% (TNF, 1—5). Fig. 2 shows the $\eta^{1/2}$ versus $(I{\cdot}t)$ on the logarithmic scale for the optimal spatial frequency for the hologram storage. Here, I is the light intensity, and t is the exposure time. The increase in the holographic sensitivity is observed when the acceptor TNF was replaced by compounds 1, 2, 5, 3, 4 (Fig. 2) in the PEPC films, and this correlates with the increase in the optical absorption at the laser wavelength.

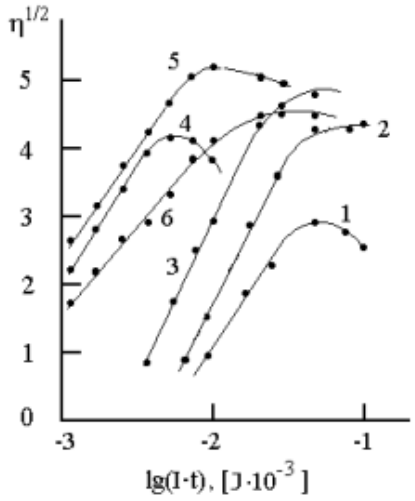

Fig. 2. $\eta^{1/2}$ versus $\lg(I \cdot t)$ for the RM based on the films made of PEPC with 1 mol.% TNF (*1*), 1 (*2*), 2 (*3*), 3 (*4*), 4 (*5*), 5 (*6*)

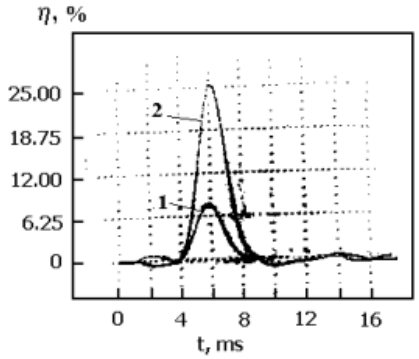

Fig. 3. Oscillogram of the development of the hologram of the RM with the PEPC + 1 mol.% (compound 5) film without precharging the polymer film surface in a corona discharge (curve *1*) and for the consistent regime (curve *2*)

The hologram storage was made with ratio of intensities of the reference and signal beams in the region from 1:1 up to 1000:1. The standard procedure [1] was used for the measurements of S, $\Delta\omega$, and ω_{opt}. In all the range of spatial frequencies, which is defined as an angle between the light beams, the holograms of the plane wave front with different exposures were registered. Then the image becomes to develop. During the process of development, the diffraction efficiency of the plane wave front hologram restored image was measured continuously. This is give a possibility to detect the maximal value of the diffraction efficiency. By the results of these measurements, the dependence of the diffraction efficiency on the exposure was detected. Using this dependence, the holographic sensitivity was defined as the value inversely proportional to the exposure which corresponds to 1% diffraction efficiency. The optimal spatial frequency range was defined according to [1]. The values $\Delta\omega$=200÷1500 mm^{-1} and ω_{opt}=350÷1000 mm^{-1} defined in this way did not vary when TNF was replaced by compounds 1—5. These values are close to the similar values for a PEPC-based RM [2]. During the multiple hologram storage and recover cycles (more than 400), the main characteristics are not decreased. The signal/noise ratio of the recovered images was at least 100. The best results were obtained for the RM based on PEPC + 1 mol.% (4). We get the maximal values η=24÷27%, $S = 30 \div 40$ m^2/J when the ratio of intensities of the reference and signal beams was 1:1.

A peculiarity of the RM based on the PEPC + 1 mol.% (1—5) films consists in the possibility to create a latent image without a polymer film preliminary charging in the corona discharge, as against to the RM based on the PEPC + 1 mol.% (TNF, 1, 2) films. With the consistent hologram storage process, the RM is charged in the corona discharge to accumulate the electrical charge on the free surface of a polymer film before the illumination, as shown above. After that, the RM is illuminated for some time without charging. The hologram latent image can be registered as a modulated signal from the free polymer film surface. But, in the case of the PEPC + 1 mol.% (3, 5) RM films, it isn't necessary to make the preliminary charging. After long-time exposure in darkness, the RM is illuminated for the hologram storage. Then the illumination is switched off, and, after some delay, the RM is charged with the corona discharge. By switching off the corona discharge, we apply a current pulse to the electroconductive sublayer for heating the polymer film up to a certain temperature for the hologram development. This gives a possibility to observe the hologram restored latent image. It means that, in such RM, the hologram restored latent image is formed only by the modulated light and keeps for a long time. Such a phenomenon corresponds to the long-time EHP photogeneration in the RM based on PEPC + 1 mol.% (1—5) films. On the other hand, it is possible to store 2 hologram images in such RM for different times and to develop both of them at the same time.

Fig. 3 shows the flat wave front development oscillogram for the RM based on a PEPC +1 mol.% (5) film, which was stored without preliminary charging of the polymer film surface in the corona discharge. For the RMs based on the PEPC with compounds 3 and 4, we get the same pictures. To develop the hologram,

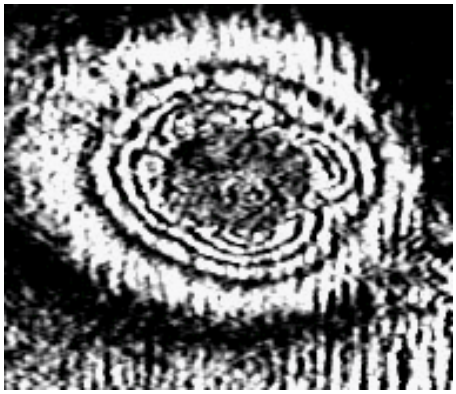

Fig. 4. The interferogram photograph of a circular defect 0.3 mm in diameter on the surface of a thick steel plate which was obtained within the double-exposure method for the RM based on the PEPC + 1 mol.% (compound 3)

the reference beam was used, after the 60-s finishing exposure. The exposure time was 30 s, and its increase doesn't increase η strongly. It should be marked that the polymer film was fresh-prepared, and it was not used before to the storage of holograms. After the hologram develops, it is erased. The repeated development of the oscillogram corresponds to the zero level, which means that the hologram was erased completely. Such storage and erase cycles are reproduced with 10% precision. Curve *2* in Fig. 3 shows the oscillogram of the development of a plane wave front hologram, which is stored with pre-charging the polymer film in a corona discharge. One can see that the maximal diffraction efficiency of the stored hologram is higher than that in the previous case. But when the temperature of the geometric relief generation is reached, the maximal diffraction efficiencies in the first and second cases of the hologram storage become equal. The results in this case are reproducible with at least 10% precision. This means that, in both the previous cases, the temperature of the polymer film RM, which corresponds to the full elimination of the preliminarily created latent image, is reached.

Fig. 3 shows the interferogram photos which were got with the double-exposure method for the RM based on a PEPC + 1 mol.% (3) film. There is no problem to obtain the same interferograms for the RM based on PEPC with compounds 4 and 5. The first hologram was stored without precharging of the polymer film surface in the corona discharge. The exposure time was 30 s, but increasing the exposure time doesn't give a huge increase in η. The polymer film was fresh-prepared and was not used before in the hologram storage. The time before the first exposure and the second one, when mechanical defects appear in the sample under investigation, was 60 s.

We may assume that the effect of latent image creation and storage in the RM based on PEPC with compounds 3—5 is equal to that in the photorefractive media [10, 11] and is related to the EHP generation with a long recombination time. As was shown earlier [2, 12, 13], the EHP life-time in the PEPC with CICT compounds films can come to 10—100 s at room temperature because of the positive potential barrier for the hole transfer from the PEPC carbazole part to the CICT molecule during the EHP annihilation and mostly for the EHP spin triplet state. Furthermore, the PEPC film contains hole traps near to the CICT molecules [14, 15], which also promotes the formation of the latent image, when they catch the photogeneration holes.

To check the proposed idea of the EHP generation in the PEPC films with compounds 2, 3, and 5 with the life-time higher than the EHP life-time in the PEPC with TNF and compounds 1, 2, we have to carried out additional investigations. These investigations were done for the sandwich-structure samples: glass substrate — SnO_2:In_2O_3—polymer film PEPC + 1 mol.% (TNF, 1—5)—Al. Aluminum films were deposited with the thermal sputtering in a vacuum camera. The thickness of Al was 0.3—0.35 μm. Using the photoresistance regime, the photo current density (j_{ph}) was measured during the illumination of the sample with the wavelength λ=633 nm from the transparent SnO_2:In_2O_3 electrode side. The electric field strength was taken within the range $E = 2{\cdot}10^7 \div 3{\cdot}10^8$ V/m. The concentrations of charge carriers Q, which were created in the electrically abridged sample in the monochromatic light time illumination interval (t_1), and carriers, which came to the collecting contacts after applying the electric field (t_2) which was started after the light pulse, were measured. To calculate Q, the well-known procedure [2] was used. It is described by the formula

$$Q = \int_0^\infty dt(i_2(t) - i_1(t))/eSL, \qquad (1)$$

where the time moment $t = 0$ corresponds to switching on the electric field, e is the electron charge, S and L are, respectively, the area and thickness of the polymer film which is placed between the contacts, $i_1(t)$ is the charging current of a sandwich-structure sample used as an electrical capacitor which was in the abridged state during the time $t_1 + t_2$ in darkness, and $i_2(t)$ is the charging current of a sandwich-structure sample used as

an electrical capacitor which was in the abridged state, illuminated by a monochromatic light within the time t_1, and then hold out in darkness.

For all the samples, photocurrent was registered. The plots of $\lg j_{\rm ph}(E)$ versus $E^{1/2}$ are linear. The slope tangents on all the graphs for all the investigated samples are the same. Thus, we may assume that, for the investigated films made from PEPC with TNF and compounds 1—5, the $j_{\rm ph}(E)$ dependence can be present as $j_{\rm ph}(E) \sim \exp(-(W_{0\rm ph} - \beta E^{1/2}))(T^{-1} - T_0^{-1})/k_{\rm B}$, which characterizes the photogeneration of charge carriers in the PEPC at the photogeneration centers (2, 4). Here, $W_{0\rm ph}$ is the activation photogeneration energy which is equal to the Coulomb attraction energy between a hole and an electron of the generated EHP, $k_{\rm B}$ is the Boltzmann constant, and T_0 is a characteristic temperature equal to 490±20 K for the PEPC film. The value of β is calculated from the $j_{\rm ph}(E)$ dependence in the logarithmic coordinates against $E^{1/2}$ as $(4.3 \pm 0.3)\cdot 10^{-5}$ eV·(V/m)$^{-1/2}$, which corresponds to the theoretical Poul—Frenkel constant (2, 4). This means that the above-discussed model of photogeneration of a EHP and its dissociation is valid for all the investigated polymer films. However, some basic differences exist in the behavior of $Q(t_1, t_2)$ for the films made of PEPC with TNF and compounds 1 and 2 as compared to that for the films made of PEPC with compounds 2, 3, and 5.

For the samples based on PEPC with TNF and compounds 1 and 2, the plots of $i_2(t)$ and $i_1(t)$ are equal, and Q is near zero. For the samples based on PEPC with compounds 3—5, Q is different from zero, and it is different for different samples. Fig. 4 shows the normalized plots of $Q(t_1)$ and $Q(t_2)$. The time of increase in Q is smaller than the relaxation time after the switch-off of light. The time of increase in Q doesn't depend on the stimulated light intensity; it is different for different samples and is close to the formation and relaxation times of a latent image for the 1st hologram storage, when the double-exposure method is used for the interferogram storage in a RM based on PEPC with compounds 3—5.

The obtained results explain the main differences between RM based on the films made of PEPC with TNF and compounds 1 and 2 and those based on films made of PEPC and compounds 3—5. The photogeneration centers in the films made of PEPC + TNF and compounds 1 and 2 are the intermolecular and intramolecular CCT between carbazole (Cz) of PEPC and TNF (Cz...TNF) and between Cz and substituted fluorene fragments (Cz...A) of molecules 1 and 2, respectively. Such centers for films made of compounds

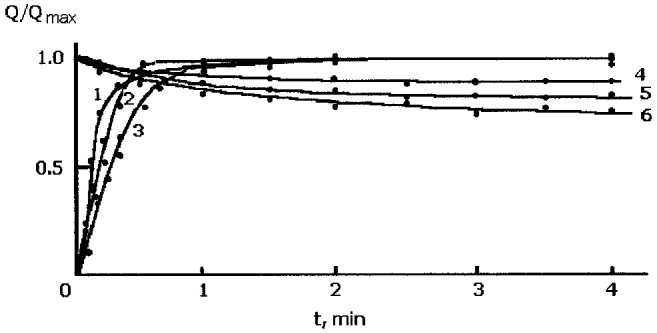

Fig.5. The dependences of the $Q/Q_{\rm max}$ on t_1 (1—3) and $Q/Q_{\rm max}$ on t_2 (4—6) for the sandwich-structure samples based on the PEPC with the 1 mol.% compound 3 (*1, 4*), 4 (*2, 5*), 5 (*3, 6*) films

3—5 (D—A) are the conjugated donor (3H-indolium) and acceptor (dicyan groups) fragments of molecules. The mechanism of photogeneration of charge carriers for the investigated RM for the latent image generation can be demonstrated by the following schemes:

$$\mathrm{Cz} + (\mathrm{Cz}\ldots\mathrm{TNF}) \xrightarrow{h\nu}$$

$$\xrightarrow{h\nu} \mathrm{Cz} + (\mathrm{Cz}^{+\cdot}\ldots\mathrm{TNF}^{-\cdot}) \rightarrow \mathrm{Cz}^{+\cdot} + (\mathrm{Cz}\ldots\mathrm{TNF}^{-\cdot}), \quad (2)$$

$$\mathrm{Cz} + (\mathrm{Cz}\ldots\mathrm{A}) \xrightarrow{h\nu}$$

$$\xrightarrow{h\nu} \mathrm{Cz} + (\mathrm{Cz}^{+\cdot}\ldots\mathrm{A}^{-\cdot}) \rightarrow \mathrm{Cz}^{+\cdot} + (\mathrm{Cz}\ldots\mathrm{A}^{-\cdot}), \quad (3)$$

$$\mathrm{Cz} + (\mathrm{D}-\mathrm{A}) \xrightarrow{h\nu} \mathrm{Cz} + (\mathrm{D}^{+}-\mathrm{A}^{-}) \rightarrow \mathrm{Cz}^{+\cdot} + (\mathrm{D}^{\cdot}-\mathrm{A}^{-}). \quad (4)$$

The hole ($\mathrm{Cz}^{+\cdot}$) photogeneration takes place when the valent electron transits from the carbazole of a PEPC fragment to the donor part of a photogeneration center. Then the anion-radical ($\mathrm{Cz}\ldots\mathrm{TNF}^{-\cdot}$) or ($\mathrm{Cz}\ldots\mathrm{A}^{-\cdot}$) is generated according to schemes (2), (3), respectively, or ($\mathrm{D}^{\cdot}-\mathrm{A}^{-}$) is created by scheme (4).

On the second photogeneration stage, a hole can recombine with an electron at the same photogeneration center, where it was before [the geminal recombination by schemes (5)—(7)],

$$\mathrm{Cz} + \ldots + \mathrm{Cz} + \mathrm{Cz}^{+\cdot} + (\mathrm{Cz}\ldots\mathrm{TNF}^{-\cdot}) \xrightarrow{-e}$$

$$\xrightarrow{-e} \mathrm{Cz} + \ldots + \mathrm{Cz} + \mathrm{Cz} + (\mathrm{Cz}\ldots\mathrm{TNF})* \rightarrow$$

$$\rightarrow \mathrm{Cz} + \ldots + \mathrm{Cz} + \mathrm{Cz} + (\mathrm{Cz}\ldots\mathrm{TNF}), \quad (5)$$

$$\mathrm{Cz} + \ldots + \mathrm{Cz} + \mathrm{Cz}^{+\cdot} + (\mathrm{Cz}\ldots A^{-\cdot}) \xrightarrow{-e}$$

$$\xrightarrow{-e} \mathrm{Cz} + \ldots + \mathrm{Cz} + \mathrm{Cz} + (\mathrm{Cz}\ldots\mathrm{A})^{*} \rightarrow$$

$$\rightarrow \mathrm{Cz} + ... + \mathrm{Cz} + \mathrm{Cz} + (\mathrm{Cz} \ldots \mathrm{A}), \quad (6)$$

$$\mathrm{Cz} + ... + \mathrm{Cz} + \mathrm{Cz}^{+\cdot} + (\mathrm{D}^{\cdot} - \mathrm{A}^{-}) \xrightarrow{-e}$$

$$\xrightarrow{-e} \mathrm{Cz} + ... + \mathrm{Cz} + \mathrm{Cz} + (\mathrm{D} - \mathrm{A})^{*} \rightarrow$$

$$\rightarrow \mathrm{Cz} + ... + \mathrm{Cz} + \mathrm{Cz} + (\mathrm{D} - \mathrm{A}) \quad (7)$$

or can move away from the electron by the transition between carbazoles [the EHP dissociation by schemes (8)—(10)]:

$$\mathrm{Cz} + ... + \mathrm{Cz} + \mathrm{Cz}^{+\cdot} + (\mathrm{Cz} \ldots \mathrm{TNF}^{-\cdot}) \xrightarrow{-e}$$

$$\xrightarrow{-e} \mathrm{Cz} + ... + \mathrm{Cz}^{+\cdot} + \mathrm{Cz} + (\mathrm{Cz} \ldots \mathrm{TNF}^{-\cdot}) \xrightarrow{-e}$$

$$\xrightarrow{-e} \mathrm{Cz}^{+\cdot} + ... + \mathrm{Cz} + \mathrm{Cz} + (\mathrm{Cz} \ldots \mathrm{TNF}^{-\cdot}), \quad (8)$$

$$\mathrm{Cz} + ... + \mathrm{Cz} + \mathrm{Cz}^{+\cdot} + (\mathrm{Cz} \ldots \mathrm{A}^{-\cdot}) \xrightarrow{-e}$$

$$\xrightarrow{-e} \mathrm{Cz} + ... + \mathrm{Cz}^{+\cdot} + \mathrm{Cz} + (\mathrm{Cz} \ldots \mathrm{A}^{-\cdot}) \xrightarrow{-e}$$

$$\xrightarrow{-e} \mathrm{Cz}^{+\cdot} + ... + \mathrm{Cz} + \mathrm{Cz} + (\mathrm{Cz} \ldots \mathrm{A}^{-\cdot}), \quad (9)$$

$$\mathrm{Cz} + ... + \mathrm{Cz} + \mathrm{Cz}^{+\cdot} + (\mathrm{D}^{\cdot} - \mathrm{A}^{-}) \xrightarrow{-e}$$

$$\xrightarrow{-e} \mathrm{Cz} + ... + \mathrm{Cz}^{+\cdot} + \mathrm{Cz} + (\mathrm{D}^{\cdot} - \mathrm{A}^{-}) \xrightarrow{-e}$$

$$\xrightarrow{-e} \mathrm{Cz}^{+\cdot} + ... + \mathrm{Cz} + \mathrm{Cz} + (\mathrm{D}^{\cdot} - \mathrm{A}^{-}). \quad (10)$$

The EHP dissociations (8)—(10) are the same for the all types of photogeneration, because the electron transitions occur between Cz and Cz^{+}, which is a part of the PEPC structure. The recombination schemes (5) and (6) are the same for the intermolecular CCT (Cz... TNF) and intramolecular complexes (Cz... A) because of the electron transfer between carbozoles from the photogeneration centers and Cz^{+} which appear in the PEPC structure. The energy barrier for such electron transitions is minimal, and the higher the recombination rate, the smaller the life-time of a EHP. For the recombination scheme (7), the electron transits from the $(\mathrm{D}^{\cdot}-\mathrm{A}^{-})$ donor part to Cz^{+} which appear in the PEPC structure. In this case, the energy barrier for the electron transitions can be bigger, and the EHP life-time increases according to the previous case.

Conclusion

Thus, the RM based on PEPC films, in which the donor and acceptor fragments are conjugated by the system of π-bonds, can be used as photogeneration centers. They have a narrow intense absorption band in the visible spectral range. Their main informational characteristics aren't worse than those of the well known model RM based on PEPC [2]. In such RM, the latent electrostatic image is generated under charging the polymer film surface with a corona discharge and during the exposure time. In this case, we succeeded to reach the high RM optical homogeneity and the transfer's linearity. The signal/noise ratio and the working periodicity of the RM are defined by the thermoplastic and rheological properties of the polymer matrix.

1. *Collier R.J., Burckhart C.B., Lin L.H.* Optical Holography. — New York and London: Academic Press, 1973.
2. *Kuvshinsky N.G., Davidenko N.A., Komko V.M.* Physics of Amorphous Molecular Semiconductors. —Kyiv: Lybid', 1994 (in Russian).
3. *Schaffert R.M.* Electrophotography. — New York: Wiley, 1981.
4. *Pope M., Swenberg C.E.* Electronic Processes in Organic Crystals. — Oxford: Clarendon Press, 1982.
5. *Freimanis Ya.F.* Organic Compounds with Intramolecular Charge Transfer. — Riga: Zinatne, 1985 (in Russian).
6. *Mysyk D.D., Perepichka I.F., Perepichka D.F. et al.* // J. Org. Chem. — 1999. — **64**, N19. — P.6937.
7. *Ishchenko A.A.* Structure and Spectral Luminescent Properties of Polymethine Dyes. — Kyiv: Naukova Dumka, 1994 (in Russian).
8. *Panasuk L.M., Nastas A.M.* // Opt. Spektr. — 2003.— **94**, N6.— P.1025.
9. *Kuvshinsky N.G., Davidenko N.A., Reshetnyak V.V. et al.* // Chem. Phys. Lett. — 1990. — **165**, N4. — P.323.
10. *Derzhypolskyy A., Melenevskyy D., Gnatovskiy A., Medved N.* // Functional Materials (submitted).
11. *Vannikov A.V., Grischina A.D.* // Uspekhi Khim. — 2003. — **72**, N6. — P.531.
12. *Davidenko N.A., Kuvshinsky N.G.*// J. Inf. Rec. Mats.— 1993. — **21**. — P. 185.
13. *Davidenko N.A., Kuvshinsky N.G.*// Ibid. — 1994. — **22**. — P.37.
14. *Davidenko N.A., Kadashchuk A.K., Kuvshinsky N.G. et al.* // Ibid. — 1996. — **24**. — P.327.
15. *Davidenko N.A., Studzinski S.L., Derevyanko N.A. et al.* // Semiconductors. — 2002. —**36**, N10. — P.1169.

ГОЛОГРАФІЧНІ
ФОТОТЕРМОПЛАСТИЧНІ СЕРЕДОВИЩА
НА ОСНОВІ ДОНОРНО-АКЦЕПТОРНИХ СИСТЕМ

М.О. Давиденко, О.О. Іщенко, Л.І. Костенко, М.Г. Кувшинський, Д.А. Меленевський, Д.Д. Мисик, Р.Д. Мисик, В.О. Павлов, М.Г. Чуприна

Р е з ю м е

Досліджено основні інформаційні характеристики нових голографічних реєструючих фототермопластичних середовищ на основі плівок полі-N-епоксипропілкарбазолу та органічних сполук з внутрішньо- і міжмолекулярним переносом заряду. Сполуки з внутрішньомолекулярним переносом заряду від донора до акцептора по системі π-зв'язків забезпечують більшу голографічну чутливість і селективність поглинання ніж сполуки, для яких перенос заряду відбувається через простір. У цих реєструючих середовищах виявлено і пояснено ефект тривалого збереження прихованого зображення до проявлення голограми.